

# Curvature Instability of Membranes near Rigid Inclusions

S. Alex Rautu<sup>1,\*</sup>

<sup>1</sup>Simons Centre for the Study of Living Machines,

National Centre for Biological Sciences (TIFR), Bellary Road, Bangalore 560065, India

(Dated: April 28, 2022)

In multicomponent membranes, internal scalar fields may couple to membrane curvature, thus renormalizing the membrane elastic constants and destabilizing the flat membranes. Here, a general elasticity theory of membranes is considered that employs a quartic curvature expansion. The shape of the membrane and its deformation energy near a long rod-like inclusion are studied analytically. In the limit where one can neglect the end-effects, the nonlinear response of the membrane to such inclusions is found in exact form. Notably, new shape solutions are obtained when the membrane is curvature unstable, manifested by a negative bending rigidity. Near the curvature instability point (i.e. at vanishing rigidity), the membrane is stabilized by the quartic curvature term, giving rise to a new length scale as well as new scale exponents for the shape and its incurred energy profile.

PACS numbers: 87.16.D-, 87.15.K-, 46.70.Hg, 68.55.-a, 46.25.Cc

Each living cell, including their organelles, is bounded by a sac-like membrane that plays an active and crucial role in almost every cellular process [1]. In its most basic form, a biomembrane consists of a bilayer structure that acts as a platform for a myriad of other biological macromolecules [2, 3]. Especially, a multitude of proteins can be incorporated into (or absorbed onto) membranes, resulting in a number of biological functions [1]. Despite their complexity, biomembranes show a clear separation of scales due to their small thickness (about 5 nm) in comparison with their lateral extent (50 nm to 100  $\mu$ m). Consequently, a large-scale theory of membranes can be constructed by means of an effective free-energy density, defined on a two-dimensional surface  $\mathcal{S}$  [4]. In particular, the deformations of a membrane near a rigid inclusion can be represented by a few local fields that live on the surface domain  $\mathcal{S}$ , e.g. the mid-plane of the bilayer, the membrane thickness, the lipid tilt, and the concentration difference between the two membrane leaflets [5–17].

In the simplest case, the membrane elasticity can be described solely in terms of geometrical quantities, where the associated free-energy  $\mathcal{H}$  is given by an expansion to second order in the surface invariants of  $\mathcal{S}$ , such as the area  $\int dS$ , the mean curvature  $H$ , and the Gaussian curvature  $K$ , which yields the *Helfrich Hamiltonian* [4]:

$$\mathcal{H}[\mathcal{S}] = \int_{\mathcal{S}} dS \left[ \sigma + \frac{\kappa}{2} (2H - C_0)^2 + \bar{\kappa} K \right], \quad (1)$$

where  $\sigma$  is the surface tension,  $C_0$  is the spontaneous curvature,  $\kappa$  is the bending rigidity, and  $\bar{\kappa}$  is the Gaussian curvature modulus. At equilibrium, the membrane shape  $\mathcal{S}$  chooses the form that minimizes its associated free-energy in Eq. (1), and subject to some other constraints, if any (e.g. a fixed difference in area of the two membrane leaflets [18], or a constant enclosed volume in the case of vesicles [19]). Such minimization leads to an Euler-Lagrange equation (known as *the shape equation*), which is a highly nonlinear partial differential equation of fourth

order [20]. In general, the latter is difficult to solve, and only a few exact solutions are known [21]. On the other hand, numerical methods have revealed more intricate surfaces, such as the biconcave shape of red blood cells [22–24], as well as non-axial symmetric vesicles [24–26].

In this Letter, a new theoretical method is developed that allows us to determine the exact nonlinear response of a membrane to the inclusion of a long rigid object, such as an adsorbed actin bundle on the membrane, as shown in Fig. 1. Firstly, we show how this analytical approach is used to obtain an exact solution to the shape equation of a Monge parametrized membrane, based on the Helfrich theory in Eq. (1). This nonlinear solution allows one to compute properties of biological relevance, which are also experimentally measurable. This includes

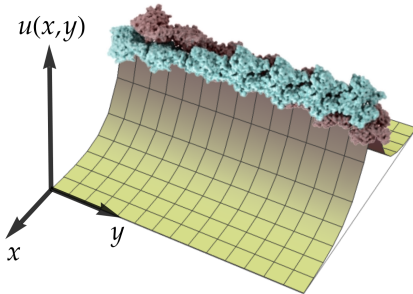


FIG. 1. (color online) Diagram of a quasi-one-dimensional fluid membrane in the vicinity of a rigid inclusion that is infinitely long in one direction, which we denote by the  $y$ -axis. This inclusion induces a shape deformation of the membrane along the  $x$ -axis. Herein, the membrane geometry is described within a Monge representation, where its surface is given by a height function  $u(x, y)$  above a flat reference plane. As a biological example, this may describe the membrane deformation close an actin bundle adsorbed on its surface, as illustrated in the figure. For clarity, the membrane that envelops the actin bundle is not shown, and only the surrounding membrane is displayed here. The rigid inclusion fixes the contact angle at the interface between the outer and the adhered membrane.

the membrane shape, and its deformation energy, beyond the linearized regime previously studied [11–17, 27–30]. In the linearized case, the membrane is approximated as a small deviation from flatness, and its shape equation can be solved exactly [17]. However, the latter is inadequate to describe the deformations of highly curved membranes, which are ubiquitous in living cells [1]. Secondly, we show that other internal degrees of freedom, emerging in the case of multi-component membranes, can also be included in this framework. These can couple to the mean curvature, and may destabilize flat membranes [31]. To further investigate the morphology of the membrane near this instability, a more general elasticity theory is considered, that employs a quartic curvature expansion [32–34], as well as the energetic cost due to compositional fields [17]. Using the same technique as before, the shape equation of a symmetric membrane can be solved analytically. Here, the quartic curvature modulus results in an entirely new physics, and notably it provides us with new exact solutions to a curvature unstable membrane.

As depicted in Fig. 1, the rigid inclusion is much longer in the  $y$ -axis than the  $x$ -axis, resulting in a membrane with translational invariance in the limit that the end-effects can be ignored. We seek its ground-state solution when the membrane is asymptotically flat. This gives the shape in terms of a height function  $u(x)$  and the distance  $x$  away from the inclusion [35]. Although the system is effectively quasi-one-dimensional, it can be shown that its associated solution to the membrane shape yields the correct (and asymptotically exact) far-field behavior of a membrane deformed in response to a circular rigid inclusion [36], such as a transmembrane protein [11].

Using Eq. (1), the effective free-energy *per unit length* of such a quasi-one-dimensional membrane is given by  $\mathcal{F}[u(x)] = \int dx f(x)$ , with the free-energy density being

$$f(x) = \hat{\sigma} \sqrt{1+u'(x)^2} + \frac{C_0 u''(x)}{1+u'(x)^2} + \frac{\frac{1}{2} \kappa u''(x)^2}{[1+u'(x)^2]^{5/2}}, \quad (2)$$

where the isotropic tension  $\hat{\sigma} = \sigma + \kappa C_0^2/2$ . Hereinafter, the dash and double-dash symbols denote the first and the second derivative with respect to the argument of a function, respectively. Eq. (2) is derived by using that the area element is  $dS = dx dy \sqrt{1+u'(x)^2}$ , the mean curvature is  $H = -\frac{1}{2} \frac{\partial}{\partial x} [u'(x)/\sqrt{1+u'(x)^2}]$ , and the Gaussian curvature  $K = 0$ . By standard variational methods, the Euler-Lagrange equation of  $\mathcal{F}[u(x)]$  is found to be [37]:  $\frac{d^4 u}{dx^4} = \frac{[1+u'(x)^2]u''(x)}{\lambda^2} + \frac{5[1-6u'(x)^2]u''(x)^3}{2[1+u'(x)^2]^2} + \frac{10u'(x)u''(x)}{1+u'(x)^2} \frac{d^3 u}{dx^3}$ , where  $\lambda = \sqrt{\kappa/\hat{\sigma}}$ . By defining  $v(x) = u'(x)$  in the above equation, and then by assuming that  $v'(x)$  is only a function of  $v(x)$ , i.e.  $Q(v) = v'(x)^2$ , this ansatz yields [37]:

$$Q''(v) = \frac{2(1+v^2)}{\lambda^2} + \frac{5(1-6v^2)Q(v)}{(1+v^2)^2} + \frac{10vQ'(v)}{1+v^2}. \quad (3)$$

This differential equation can be solved by seeking a solution of the form  $Q(v) = (1+v^2)^{5/2} P(v)$ , where  $P(v)$

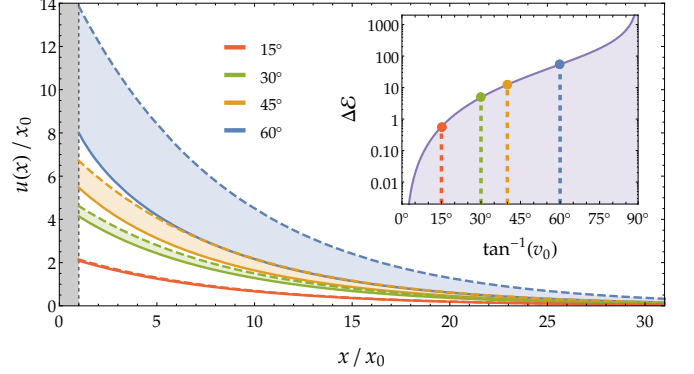


FIG. 2. (color online) Membrane profiles near an inclusion for a few values of the contact angles. The spontaneous curvature  $C_0 = 0$ , and  $x_0 = 1$  nm and  $\lambda = 8$  nm, which are physiologically reasonable values. The solid curves represent the exact solutions from Eq. 7, while the dashed curves are their corresponding linearized versions. The inset shows the absolute integrated error  $\Delta\mathcal{E}$  (i.e. the shaded area between the solid and dashed curves) as a function of the contact angle.

is some function. By substituting this form into Eq. (3), this reduces to  $P''(v) = 2\lambda^{-2} (1+v^2)^{-3/2}$ , which can be solved by a method of variation of parameters [38]. As a result, the general solution of Eq. (3) is given by

$$Q(v) = 2\lambda^{-2} (1+v^2)^3 + (\mathcal{C}_1 + v\mathcal{C}_2) (1+v^2)^{5/2}, \quad (4)$$

where  $\mathcal{C}_1$  and  $\mathcal{C}_2$  are constants of integration, which are fixed by the boundary conditions that the membrane becomes flat only at distances far from the inclusion. This asymptotic flatness can be imposed by requiring that both  $Q(v)$  and its derivative  $Q'(v)$  vanish in the limit of  $v \rightarrow 0$ , which yields that  $\mathcal{C}_1 = -2\lambda^{-2}$  and  $\mathcal{C}_2 = 0$ .

By chain rule, we have that  $v(x) = v'(x)u'(v)$ , then the membrane height as a function of  $v$  is given by

$$u(v) = \pm \int_0^v d\nu \frac{\nu}{\sqrt{Q(\nu)}} = \pm \lambda \sqrt{2 - \frac{2}{\sqrt{1+v^2}}}, \quad (5)$$

where we use the boundary condition that  $u(v \rightarrow 0) = 0$ . Also, at the interface between the rigid inclusion and the membrane, we choose the contact angle to be given by  $v_0$ , which sets the height at the inclusion to be  $u_0 = u(v_0)$ . Thus, by inverting Eq. (5), the gradient  $v$  is written as

$$v(u) = \pm u \sqrt{4\lambda^2 - u^2} / (2\lambda^2 - u^2) = u'(x), \quad (6)$$

where  $|u| < \lambda\sqrt{2}$  is required to invert Eq. (5), setting an upper bound on the size of the membrane height. Since the region spanned by the rigid inclusion is chosen to be the interval  $[-x_0, x_0]$ , with  $x_0 \geq 0$ , then Eq. (6) can be integrated to find the position  $x$  of the outer membrane as a function of  $u$ , i.e.  $x(u) = \pm [x_0 + \mathcal{X}(u_0) - \mathcal{X}(u)]$ , with  $\mathcal{X}(u) = \sqrt{4\lambda^2 - u^2} - \lambda \operatorname{arccosh}(2\lambda/|u|)$ . The minus sign represents the negative regime with  $x \in [-x_0, -\infty)$ ,

whilst the plus sign corresponds to  $x \in [x_0, \infty)$ . Thus, the solution for the membrane height can be written as

$$|u| = 2\lambda \operatorname{sech} \left[ \sqrt{4 - u^2/\lambda^2} - [x_0 - |x| + \mathcal{X}(u_0)]/\lambda \right], \quad (7)$$

with  $\operatorname{sech}$  as the hyperbolic secant [39]. Typical membrane profiles are shown in Fig. 2. The linearized solution [17] can be retrieved by expanding Eq. (7) to lowest order in  $u$  and  $u_0$ , yielding  $u(x) \simeq \pm u_0 e^{-(|x|-x_0)/\lambda}$  and  $u_0 \simeq v_0 \lambda$ . This allows us to estimate the error in approximating the membrane as a small deviation from flatness, as shown in Fig. 2. This gives us an upper bound for the contact angle at which the linearized solution is a good approximation, which is found to be about  $10^\circ$  and  $20^\circ$  at 1% and 5% maximal relative error, respectively [40].

Once the membrane shape is determined, the deformation energy can be computed analytically. The energetic cost per unit length to deform a membrane from flatness is given by  $\Delta\mathcal{F} \equiv \mathcal{F}[u] - \mathcal{F}[0] = 2 \int_{x_0}^{\infty} dx [f(x) - \hat{\sigma}]$ . By using Eq. (6),  $f$  can be rewritten as a function of  $u$  only. Hence, the integral can be evaluated exactly by a change of variables, i.e.  $dx = x'(u) du$ , which yields:

$$\Delta\mathcal{F} = 4\sqrt{\kappa\hat{\sigma}} \left[ 2 - \sqrt{4 - \frac{u_0^2}{\lambda^2}} + \lambda C_0 \csc^{-1}(2\lambda/u_0) \right], \quad (8)$$

where  $\csc^{-1}$  is the inverse cosecant. In the small angle approximation (linearized case), the deformation energy reduces to  $\Delta\mathcal{F} \simeq \sqrt{\kappa\hat{\sigma}} (v_0^2 + 2v_0\lambda C_0)$ , as  $u_0 \simeq v_0\lambda$ . The dependences of  $\Delta\mathcal{F}$  on  $v_0$  and  $C_0$  are shown in Fig. 3.

So far, only the energetics incurred by membrane shape deformations have been considered. However, other fields that live on the surface  $\mathcal{S}$  can be taken into account [31]. In the case of a mixed two-component lipid membrane, the local relative concentration between the leaflets of the membrane, say  $\varphi$ , incurs an energetic contribution of the form  $\mathcal{F}_\varphi[\mathcal{S}] = \int_{\mathcal{S}} dS [\frac{1}{2}a\varphi^2 + 2c\varphi H]$  to lowest order in  $\varphi$ , where  $a$  and  $c$  are phenomenological parameters [17]. By minimizing over  $\mathcal{F} + \mathcal{F}_\varphi$ , the ground state solution to  $\varphi$  for a quasi-one-dimensional membrane as shown in Fig. 1 is  $\varphi = -2cH/a$  [37]. This effectively renormalizes  $\kappa$  to a new bending modulus  $\tilde{\kappa} = \kappa[1 - c^2/(a\kappa)]$ , and thus the corresponding membrane height is found to be in a form identical to Eq. (7) where  $\lambda \mapsto \tilde{\lambda} = \sqrt{\tilde{\kappa}/\hat{\sigma}}$ . The regime  $c > \sqrt{a\kappa}$  corresponds a membrane curvature instability, known as the Leibler's unstable regime [31].

The free-energy functional in Eq. (1) is found by truncating at second-order in curvature, and assuming that higher order terms are much smaller; however, *a priori* there is no clear basis for this assumption [4]. In fact, higher-order terms become more important as the Leibler instability is approached, leading to a much softer bending modulus. To better understand its physical implications, we consider a symmetric membrane and quasi-one-dimensional as in Fig. 1. Hence, the next terms appear at fourth-order in the inverse-length, i.e.  $K^2$ ,  $KH^2$ ,  $H^4$ ,

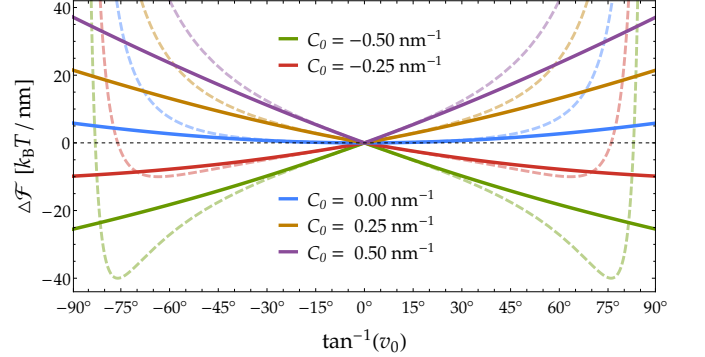


FIG. 3. (color online) The deformation free-energy per unit length  $\Delta\mathcal{F}$  for a few values of  $C_0$ . The solid line is the exact result in Eq. 8, whilst the dashed curve is the corresponding linearized energy. Here,  $\kappa = 20 k_B T$  and  $\sigma = 0.1 \text{ mN/m}$ .

and  $(\nabla_\alpha H)(\nabla^\alpha H)$  [34]. Since  $K = 0$ , the first two terms vanish identically. The last term is neglected herein, as it contains derivatives of mean curvature, introducing sub-dominant terms, and thus we only consider the  $H^4$  term.

Using the techniques developed previously, an exact solution to the shape can be found again for this quartic curvature theory of membranes, where the free-energy is  $\mathcal{H}_4[\mathcal{S}] = \int_{\mathcal{S}} dS [\sigma + 2\kappa H^2 + 4\kappa_4 H^4]$ , with  $\kappa_4 \geq 0$  as the quartic curvature modulus. As in Eq. (2), the free-energy per unit length is given by  $\mathcal{F}_4[u(x)] = \int dx f_4(x)$ , where

$$f_4 = \sigma \sqrt{1+u'(x)^2} + \frac{\frac{1}{2} \kappa u''(x)^2}{[1+u'(x)^2]^{\frac{5}{2}}} + \frac{\frac{1}{4} \kappa_4 u''(x)^4}{[1+u'(x)^2]^{\frac{11}{2}}} \quad (9)$$

represents the projected free-energy density. The shape equation of  $\mathcal{F}_4 + \mathcal{F}_\varphi$  can be found [37] and rewritten in terms of a new function  $\mathcal{Q}(v) = v'(x)^2$  as before, where  $v$  is the membrane gradient. By the condition of asymptotic flatness, both  $\mathcal{Q}(v)$  and  $\mathcal{Q}'(v)$  are required to vanish at  $v = 0$ , which yields the following two solutions [37]:

$$\mathcal{Q}_\pm(v) = \frac{4\sigma(1+v^2)^3}{\pm\tilde{\kappa}\varepsilon^2} \left[ \sqrt{1+\varepsilon^2 - \frac{\varepsilon^2}{\sqrt{1+v^2}}} \mp 1 \right], \quad (10)$$

where  $\varepsilon^2 = 12\sigma\kappa_4/\tilde{\kappa}^2$ , representing the ratio of two characteristic lengths:  $\xi = \sqrt{\kappa_4/|\tilde{\kappa}|}$  and  $\tilde{\lambda} = \sqrt{|\tilde{\kappa}|/\sigma}$ . As  $\mathcal{Q}$  must be greater than zero, only  $\mathcal{Q}_+$  solution is allowed if  $\tilde{\kappa} > 0$ . However, if the bending modulus switches sign and becomes negative, as in the case of the Leibler's instability, then only  $\mathcal{Q}_-$  must be chosen for stability.

By the flatness condition  $u(v \rightarrow 0) = 0$ , c.f. Eq. (5), the profile  $u$  can be exactly computed in terms of  $v$  [37]:

$$|u(v)| = U_\pm + \frac{\tilde{\lambda}^2 \sqrt{\mathcal{Q}_\pm(v)}}{(1+v^2)^{3/2}} \left[ \frac{\varepsilon^2 \tilde{\lambda}^2 \mathcal{Q}_\pm(v)}{12(1+v^2)^3} \pm 1 \right], \quad (11)$$

with  $U_+ = 0$  and  $U_- = 2\tilde{\lambda}\sqrt{2}/(3\varepsilon)$ . For  $\tilde{\kappa} > 0$ , Eq. (5) is retrieved when  $\varepsilon \rightarrow 0$  ( $\tilde{\lambda} \gg \xi$ ), whereas for  $\tilde{\kappa} < 0$  the

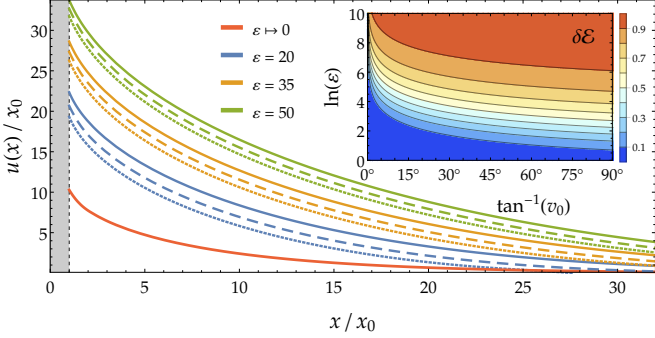


FIG. 4. (color online) Deformation profiles based on a quartic curvature theory of membranes for a few values of  $\varepsilon$  (see text). The solid and dotted lines correspond to the regimes of  $\tilde{\kappa} > 0$  and  $\tilde{\kappa} < 0$ , respectively. The dashed curves are the asymptotic solutions as  $\varepsilon \rightarrow \infty$ . Herein, the contact angle is  $80^\circ$ , while  $x_0 = 1 \text{ nm}$ ,  $\sigma = 0.1 \text{ mN/m}$ , and  $|\tilde{\kappa}| = 20 k_B T$ . The inset shows the relative error  $\delta\mathcal{E} = (u[\varepsilon] - u[\varepsilon = 0])/u[\varepsilon]$ , with  $\tilde{\kappa} > 0$  and  $x = x_0$ , as a function of  $\ln(\varepsilon)$  and the contact angle.

height  $u$  vanishes at  $\varepsilon = 0$  and its linear order term in  $\varepsilon$  gives  $|u(v)| = \xi (1 - 1/\sqrt{1 + v^2}) \sqrt{3/2}$ . On the other hand, in the asymptotic limit  $\varepsilon \rightarrow \infty$  ( $\tilde{\lambda} \ll \xi$ ), i.e. near the instability, both solutions yield the same profile, i.e.

$$|u(v)| \simeq 2^{-3/4} \Lambda \left[ 1 - 1/\sqrt{1 + v^2} \right]^{3/4} \quad (12)$$

with  $\Lambda = \frac{4}{3} \sqrt[4]{6 \kappa_4 / \sigma}$  [37]. This asymptotic form can be inverted, as in Eq. (6), if only  $|u(x)| < 2^{-3/4} \Lambda$ , hence setting an upper bound on the membrane height. Then, by integrating over  $u$ , the membrane position from the rigid inclusion (namely,  $|x| \geq x_0$  and  $|u| \leq |u_0|$ ) is found to be [37]:  $|x(u)| \simeq x_0 + \mathcal{X}_\infty(u_0) - \mathcal{X}_\infty(u)$ , where  $\mathcal{X}_\infty(u) = \frac{\Lambda}{2} \text{sn}^{-1}(\sqrt[3]{|u|/\Lambda} | - 1) + \Lambda \sqrt{(u/\Lambda)^{2/3} - (u/\Lambda)^2}$ , with  $\text{sn}^{-1}(\vartheta|m)$  as the inverse of the  $sn$  Jacobi elliptic function [41]. Rearranging as in Eq. (7), this gives the height in terms of  $|x|$ , see Fig. 4. For  $\xi \gg \tilde{\lambda}$ , we find that a small gradient  $\frac{du}{dx} \sim u^{2/3}$ , yielding the algebraic solution  $x(u) \sim u^{1/3}$ , whilst for  $\tilde{\lambda} \gg \xi$  we have  $\frac{du}{dx} \sim u$ , which leads to the logarithmic solution  $x(u) \sim \log|u|$ .

In its exact form, Eq. (11) can be re-expressed as a cubic equation in  $\mathcal{V} \equiv 1 - 1/\sqrt{1 + v^2}$ , which has only one real root. As a result, Eq. (11) can be analytically inverted for any  $\varepsilon$ , but now the inverse gradient,  $v^{-1}(u)$ , has a cumbersome expression, and its integral over  $u$  can no longer be written in a closed form [37]. Nonetheless, this can be integrated numerically, as shown in Fig. 4. When  $\tilde{\kappa} > 0$ , the maximal relative error  $\delta\mathcal{E}$  in neglecting the quartic term can be exactly computed from Eq. (11), and its result is shown in the inset plot of Fig. 4. If  $\xi = \tilde{\lambda}$ , then we need a contact angle of about  $14^\circ$  for  $\delta\mathcal{E} = 10\%$ .

Using Eqs. (10) and (11), the deformation energy from flatness  $\Delta\mathcal{F}_4$  for  $\tilde{\kappa} > 0$  can be reduced to the following simple integral [37]:  $\Delta\mathcal{F}_4 = 2\sigma \int_0^{v_0} dv u(v)/(1 + v^2)$ , which can be numerically integrated as shown in Fig. 5.

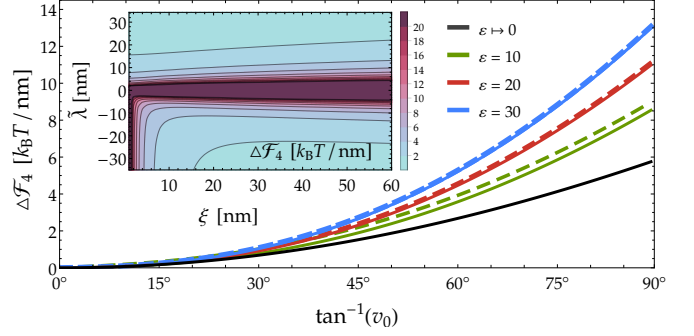


FIG. 5. (color online) The deformation free-energy per unit length,  $\Delta\mathcal{F}_4$ , in the quartic theory of membranes (see text). By setting  $\sigma = 0.1 \text{ mN/m}$ ,  $\Delta\mathcal{F}_4$  versus the contact angle is shown for a few values of  $\varepsilon$  when  $\tilde{\kappa} = 20 k_B T$  (solid lines) and  $\tilde{\kappa} = -20 k_B T$  (dashed lines). The inset is a density plot of  $\Delta\mathcal{F}_4$  against both  $\tilde{\lambda}$  and  $\xi$ , at a contact angle of  $80^\circ$ , where the negative values of  $\tilde{\lambda}$  correspond to  $-\sqrt{|\tilde{\kappa}|}/\sigma$  when  $\tilde{\kappa} < 0$ .

By Taylor expanding in  $\varepsilon$  about zero, this allows us to compute the lowest order contribution to the deformation energy due to the quartic term, namely  $\Delta\mathcal{F}_4 = \Delta\mathcal{F} + \frac{\tilde{\kappa}\varepsilon^2}{18\tilde{\lambda}} \left[ 8 - (5 - 1/\sqrt{1 + v_0^2}) \sqrt{2 + 2/\sqrt{1 + v_0^2}} \right] + \mathcal{O}[\varepsilon^4]$ . This result can be used to determine the values of  $\xi$  at which the  $\varepsilon^2$ -term becomes greater than  $\Delta\mathcal{F}$ . By equating these two terms, we find at the modest contact angles of  $15^\circ$  and  $30^\circ$  that  $\xi \approx 11\tilde{\lambda}$  and  $\xi \approx 5\tilde{\lambda}$ , respectively. On the other hand, the deformation energy for  $\tilde{\kappa} < 0$  takes a different form than before [37], which can be written as  $\Delta\mathcal{F}_4 = \tilde{\kappa} \int_0^{v_0} dv \frac{\varepsilon^2 \tilde{\lambda}^2 \mathcal{Q}_-(v)^{3/2}}{6(1+v^2)^{11/2}}$ , and shown in Fig. 5. Hence, its expansion in  $\varepsilon$  about zero is given by  $\Delta\mathcal{F}_4 = \frac{4\tilde{\lambda}}{3\varepsilon\sqrt{2}} \tan^{-1}(v_0) + \frac{\varepsilon\tilde{\lambda}}{2\sqrt{2}} \left[ \tan^{-1}(v_0) - \frac{v_0}{\sqrt{1+v_0^2}} \right] + \mathcal{O}[\varepsilon^3]$ . However, near the curvature instability ( $\varepsilon \rightarrow \infty$ ), we find that the same expression for the both signs of  $\tilde{\kappa}$  [37], i.e.  $\Delta\mathcal{F}_4 \simeq 2\sigma \int_0^{v_0} dv \frac{|u(v)|}{1+v^2} + \mathcal{O}[\frac{1}{\varepsilon}] \simeq \frac{\sigma\Lambda\sqrt{2}}{5} v_0^{\frac{5}{2}} + \mathcal{O}[v_0^{\frac{9}{2}}]$ , where the form of  $u(v)$  from Eq. (12) is used, and the last equality is a small  $v_0$  expansion. The full dependence of  $\Delta\mathcal{F}_4$  on both  $\tilde{\lambda}$  and  $\xi$  is shown in the inset of Fig. 5.

In summary, we computed exactly the energetics and shape of a membrane deformed by a rigid inclusion. We studied its nonlinear response in the Monge gauge by using the Helfrich Hamiltonian as well as a quartic curvature theory of membranes. The latter reveals interesting new physics; in particular, new shape solutions have been obtained above and below the curvature instability of membranes ( $\kappa = 0$ ). Near this instability, both solutions yield the same morphology and deformation energy, which are fundamentally different to those found in bulk stable membranes ( $\kappa > 0$ ). In addition, these new exact (nonlinear) results allow us to calculate bounds on the contact angle and the quartic modulus at which the usual quadratic truncations (in the membrane height and/or its curvature) are still well founded approximations.

The author acknowledges the stimulating discussions with Prof. G. Rowlands (University of Warwick, United Kingdom), Prof. M. Rao, Dr. R. Morris, and A. Singh (National Centre for Biological Sciences, India), and the funding from the Simons Foundation (United States).

\* stefanar@ncbs.res.in

[1] B. Alberts, A. Johnson, J. Lewis, M. Raff, K. Roberts, and P. Walter, *Molecular Biology of the Cell*, 5th ed. (Garland Science, New York, 2008).

[2] S. J. Singer and G. L. Nicolson, *Science* **175**, 720 (1972).

[3] D. M. Engelman, *Nature* **438**, 578 (2005).

[4] M. Deserno, *Chem. Phys. Lipids* **185**, 11 (2015).

[5] W. Helfrich, *Z. Naturforsch. C Bio. Sci.* **28**, 693 (1973).

[6] P. B. Canham, *J. Theor. Biol.* **26**, 61 (1970).

[7] H. W. Huang, *Biophys. J.* **50**, 1061 (1986).

[8] N. Dan, P. Pincus, and S. A. Safran, *Langmuir* **9**, 2768 (1993).

[9] H. Aranda-Espinoza, A. Berman, N. Dan, P. Pincus, and S. A. Safran, *Biophys. J.* **71**, 648 (1996).

[10] C. Nielsen, M. Goulian, and O. S. Andersen, *Biophys. J.* **74**, 1966 (1998).

[11] J.-B. Fournier, *Eur. Phys. J. B* **11**, 261 (1999).

[12] T. R. Weikl, M. Kozlov, and W. Helfrich, *Phys. Rev. E* **57**, 6988 (1998).

[13] P. Wiggins and R. Phillips, *Biophys. J.* **88**, 880 (2005).

[14] K. S. Kim, J. Neu, and G. Oster, *Biophys. J.* **75**, 2274 (1998).

[15] M. Goulian, R. Bruinsma, and P. Pincus, *Eur. Lett.* **22**, 145 (1993).

[16] C. A. Haselwandter and R. Phillips, *Eur. Lett.* **101**, 68002 (2013).

[17] S. A. Rautu, G. Rowlands, and M. S. Turner, *Phys. Rev. Lett.* **114**, 098101 (2015).

[18] L. Miao, U. Seifert, M. Wortis, and H.-G. Döbereiner, *Phys. Rev. E* **49**, 5389 (1994).

[19] U. Seifert, *Adv. Phys.* **46**, 13 (1997).

[20] O.-Y. Zhong-can and W. Helfrich, *Phys. Rev. Lett.* **59**, 2486 (1987).

[21] This includes Clifford tori [42], Dupin cyclides [43], non-circular cylinders [44, 45], ellipsoids [46–48], Delaunay surfaces [48–51], and a few axisymmetrical vesicles with non-constant mean curvature [51].

[22] H. J. Deuling and W. Helfrich, *Biophys. J.* **16**, 861 (1976).

[23] G. Lim H W, M. Wortis, and R. Mukhopadhyay, *Proc. Natl. Acad. Sci. USA* **99**, 16766 (2002).

[24] V. Kralj-Iglič, S. Svetina, and B. Žekš, *Eur. Biophys. J.* **22**, 97 (1993).

[25] V. Heinrich, S. Svetina, and B. Žekš, *Phys. Rev. E* **48**, 3112 (1993).

[26] Y. Jie, L. Quanhui, L. Jixing, and O.-Y. Zhong-Can, *Phys. Rev. E* **58**, 4730 (1998).

[27] K. S. Kim, J. Neu, and G. Oster, *Phys. Rev. E* **61**, 4281 (2000).

[28] M. Deserno, *Phys. Rev. E* **69**, 031903 (2004).

[29] M. M. Müller, M. Deserno, and J. Guven, *Phys. Rev. E* **76**, 011921 (2007).

[30] M. Hu, P. Diggins, and M. Deserno, *J. Chem. Phys.* **138**, 214110 (2013).

[31] S. Leibler and D. Andelman, *J. Phys. Fr.* **48**, 2013 (1987).

[32] J. B. Fournier and P. Galatola, *Eur. Lett.* **39**, 225 (1997).

[33] R. Goetz and W. Helfrich, *J. Phys. II Fr.* **6**, 215 (1996).

[34] R. Capovilla, J. Guven, and J. A. Santiago, *J. Phys. A Math. Gen.* **36**, 6281 (2003).

[35] Similar solutions have been found by means of an arc-length parametrization of the tangent angle  $\psi(s)$  [28–30], which allows for overhangs. By integrating over  $\sin \psi$  and  $\cos \psi$ , we attain the vertical and horizontal profiles of the membrane, respectively. However, one needs to numerically resolve for these to find the shape in terms of more relevant variables, e.g. the distance from the inclusion.

[36] For an axisymmetrical rigid inclusion [17], Eq. (1) can be written as  $2\pi \int dr [rf(r)]$ , with  $f$  defined in Eq. (2). The prefactor  $r$  yields an extra term in the Euler-Lagrange equation, i.e.  $g(r) \equiv r^{-1}[-\partial f/\partial u' + \frac{d}{dr}(\partial f/\partial u'')]$ , where the remaining terms are identical to those found in the quasi-one-dimensional case. As  $g(r)$  becomes negligibly small and asymptotically vanishes far from the inclusion, the leading terms yield a shape equivalent and asymptotically exact to Eq. (7). Such axisymmetrical solutions have been studied in [52] using asymptotic methods.

[37] Supplemental Material provides additional calculations, and includes Refs. [4, 17, 39].

[38] P. Denney and A. Krzywicki, *Mathematics for Physicists* (Dover Pub., New York, 1996).

[39] M. Abramowitz and I. Stegun, *Handbook of Mathematical Functions* (Dover Pub., New York, 1965).

[40] This relative error is independent of  $\lambda$ , and can be exactly derived from Eq. (5), i.e.  $\delta\mathcal{E} = v_0/\sqrt{2 - 2/\sqrt{1 + v_0^2}} - 1$ .

[41] This is defined by  $sn^{-1}(\vartheta|m) := \int_0^{\vartheta} \frac{dt}{\sqrt{1-t^2}\sqrt{1-mt^2}}$ , where the real parameters  $\vartheta \in (-1, 1)$  and  $m < 1$ .

[42] O.-Y. Zhong-can, *Phys. Rev. A* **41**, 4517 (1990).

[43] O.-Y. Zhong-can, *Phys. Rev. E* **47**, 747 (1993).

[44] Z. Shao-guang and O.-Y. Zhong-can, *Phys. Rev. E* **53**, 4206 (1996).

[45] O.-Y. Zhong-Can, L. Ji-Xing, and X. Yu-Zhang, *Geometric Methods in the Elastic Theory of Membranes in Liquid Crystal Phases* (World Scientific, Singapore, 1999).

[46] W.-M. Zheng and J. Liu, *Phys. Rev. E* **48**, 2856 (1993).

[47] Q.-H. Liu, Z. Haijun, J.-X. Liu, and O.-Y. Zhong-Can, *Phys. Rev. E* **60**, 3227 (1999).

[48] H. Naito, M. Okuda, and O.-Y. Zhong-can, *Phys. Rev. E* **48**, 2304 (1993).

[49] H. Jian-Guo and O.-Y. Zhong-Can, *Phys. Rev. E* **47**, 461 (1993).

[50] I. Mladenov, *Eur. Phys. J. B* **29**, 327 (2002).

[51] H. Naito, M. Okuda, and O.-Y. Zhong-can, *Phys. Rev. Lett.* **74**, 4345 (1995).

[52] P. Biscari and G. Napoli, *Biomech. Model. Mechanobiol.* **6**, 297 (2007).